Destabilization of Membranes Containing Cardiolipin or Its Precursors by Peptides Derived from Mitogaligin, a Cell Death Protein†

Patrick Gonzalez, Mélanie Duneau, Stéphane Charpentier, Thierry Normand, Lucile Mollet, Martine Dubois, and Alain Legrand*

Centre de Biophysique Moléculaire (Affiliated with the University of Orléans), CNRS UPR4301, Rue Charles Sadron, 45071 Orléans Cedex 2, France

Received January 31, 2007; Revised Manuscript Received April 30, 2007

ABSTRACT: *Galig*, a gene embedded within the galectin-3 gene, induces cell death when transfected in human cells. This death is associated with cell shrinkage, nuclei condensation, and aggregation of mitochondria. Galig contains two different overlapping open reading frames encoding two unrelated proteins. Previous observations have shown that one of these proteins, named mitogaligin, binds to mitochondria and promotes the release of cytochrome *c*. However, the mechanism of action of this cytotoxic protein remains still obscure. The present study provides evidence that synthetic peptides enclosing the mitochondrial localization signal of mitogaligin bind to anionic biological membranes leading to membrane destabilization, aggregation, and content leakage of mitochondria or liposomes. This binding to anionic phospholipids is the most efficient when cardiolipin, a specific phospholipid of mitochondria, is inserted in the membranes. Thus, cardiolipin may constitute a target of choice for mitogaligin sorting and membrane destabilization activity.

Programmed cell death is a crucial process controlling normal development, cellular homeostasis, tissue renewing, and elimination of neoplastic cells. The essential role of mitochondria in mediating programmed cell death has now been clearly established. Releasing of death-promoting factors from the intermembrane space of mitochondria constitutes a key step, leading subsequently to caspase's cascade activation (*1*−*3*). Members of the Bcl-2 protein family control mitochondria homeostasis and are the most well-defined regulators of the apoptotic mitochondrial pathway (*4*). Among these proteins, proapoptotic members, such as Bid and Bax or Bad and Bak, trigger this mitochondrial pathway while others, such as Bcl-2 or Bcl-XL, inhibit apoptosis in preventing release of soluble proteins from the intermembrane space. Recently, we have identified an internal gene in the human galectin-3 locus as a new cell death inducer gene (*5*). This gene, named *galig* (galectin-3 internal gene), contains two different overlapping reading frames and encodes two unrelated proteins (*6*). These proteins are distinct from galectin-3. *Galig* expression causes morphological alterations in human cells, such as cell shrinkage, cytoplasm vacuolization, nuclei condensation, and ultimately cell death. These alterations are associated with aggregation of mitochondria and extramitochondrial release of cytochrome *c*. Although not related to the Bcl-2 family, we have shown that *galig* coexpression with Bcl-xL is protective against cytochrome *c* release, suggesting a common pathway between the cytotoxic activity of *galig* and the antiapoptotic activity of Bcl-xL. This antagonism was not observed upon cotransfection of Bcl-2 and *galig* (*5*).

Previous observations have led to the conclusion that mitogaligin, one of the proteins encoded by *galig*, binds to mitochondria and promotes the release of cytochrome *c*. Mitogaligin is a 97 amino acid protein, highly cationic and exceptionally rich in tryptophan residues (12%). Structure−activity relationship experiments showed that the mitochondrial addressing of mitogaligin relies on an internal sequence, which is required for the cytosolic release of cytochrome *c* (*5*). Moreover, incubation of isolated mitochondria with peptides derived from mitogaligin induces cytochrome *c* release. However, the mechanism of action of mitogaligin leading to mitochondria permeability remains still obscure. The present results provide evidence that peptides derived from mitogaligin induce membrane aggregation and content leakage of mitochondria and anionic liposomes. This study supports a model in which mitogaligin would interact, in vivo, with cardiolipin, an anionic phospholipid of the mitochondrial membrane.

EXPERIMENTAL PROCEDURES

Expression Vectors and Cell Transfections. pMG3154-EGFP is a plasmid encoding amino acids 31−54 of mitogaligin fused to the EGFP coding sequence (*5*). Vectors encoding truncated forms of this fusion protein were generated by inverse PCR. Deletions were performed to remove one amino acid at a time starting from the N- or C-terminal ends of the mitogaligin sequence. Plasmids were checked by sequencing and transfected into HeLa cells (ATCC, CCL-

† This work was supported by grants from the Comités Départementaux d'Eure-et-Loir et du Cher de La Ligue Nationale Contre le Cancer. P.G. and M.D. are supported by fellowships from the Ministère de l'Enseignement Supérieur et de la Recherche. P.G. is also supported by a fellowship from the Association pour la Recherche sur le Cancer.

* To whom correspondence should be addressed. Tel: (33) 2 38 25 55 36. Fax: (33) 2 38 25 78 07. E-mail: legrand@cnrs-orleans.fr.

10.1021/bi700213p CCC: $37.00
Published on Web 06/05/2007

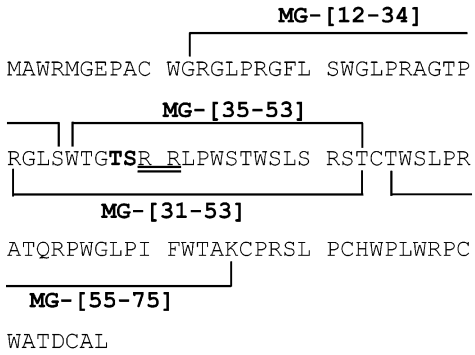

FIGURE 1: Sequences of mitogaligin and of derived synthetic peptides. Substitution of residues in bold (T38 and/or S39) with glutamate (E) in peptide MG-[35−53] generated peptides S39/E and T38S39/EE. Substitution of residues double underlined (R40 and R41) with alanines (A) generated peptide R40R41/AA.

2) using DNA−poly(ethylenimine) complexes (PEI)[1] (*7*) as described (*6*). Twenty-four hours after transfection, cells were incubated at 37 °C for 10 min with 0.1 μg/mL tetramethylrhodamine ethyl ester (TMRM; Sigma). This specific mitochondrial marker is sensitive to the potential membrane. Cells were washed with cell culture medium and analyzed by fluorescence microscopy using fluorescein filters (excitation at 488 nm and detection at 520 nm for EGFP) and rhodamine filters (excitation at 543 nm and detection 590 nm for TMRM).

Release of Cytochrome c into the Cytosol of Transiently Transfected HeLa Cells. Twenty-four hours after transfection, cells were checked by fluorescence microscopy for EGFP fusion protein production and localization. Then, cells were washed twice with PBS and incubated on ice in 250 μL of lysis buffer (250 mM sucrose, 10 mM KCl, 1.5 mM $MgCl_2$, 1 mM EDTA, 20 mM HEPES) supplemented with a cocktail of protease inhibitors (Sigma Aldrich), 1 M dithiothreitol, and 100 mM phenylmethanesulfonyl fluoride for 30 min. After homogenization in a Dounce homogenizer, homogenates were centrifuged at 15000*g* for 30 min. The pellets were incubated for 20 min on ice with 5 μL of 10% saponin and then suspended in 250 μL of lysis buffer. The suspension was centrifuged at 15000*g* for 10 min, and the protein concentration was estimated by the method of Bradford. The resulting supernatants were analyzed by immunoblotting for detection of cytochrome *c* using a murine monoclonal anti-cytochrome *c* antibody (1:250) (clone 7H8.2C12; Pharmingen, BD Biosciences, France) followed by horseradish peroxidase-conjugated secondary antibody (1:5000). The protein was detected with the ECL detection system (BM chemiluminescence western blotting kit; Roche Diagnostic) according to the manufacturer's instructions.

Synthesis of Mitogaligin-Derived Peptides. Peptides covering different regions of mitogaligin were synthesized (see sequences in Figure 1). A standard 9-fluorenylmethoxycarbonyl (Fmoc) solid-phase method was used. Peptides were assembled on an Fmoc-Rink amide aminomethyl resin using a Perkin-Elmer Applied Biosystems 431A synthesizer and subsequently cleaved from the resin with trifluoroacetic acid (82.5%) and a mixture of scavengers (thioanisole, 5%; ethanedithiol, 2.5%; phenol, 5%; and water, 5%) (*8*). Side chains were protected by 2,2,4,6,7-pentamethyldihydrobenzofuran-5-sulfonyl (Arg) or *tert*-butyl (Ser and Thr) or *tert*-butyloxycarbonyl (Trp). Peptides were purified to homogeneity by high-performance liquid chromatography using a semipreparative C18 reverse-phase column. Identities of the synthetic peptides were confirmed by MALDI-TOF mass spectrometry (*9*).

Preparation of Liposomes. All liposomes were prepared by reverse-phase evaporation. Briefly, lipids were dissolved in chloroform. The following ratios were used for zwitterionic liposomes: 20/1 for phosphatidylcholine (PC) and cholesterol (Chol), respectively.

Anionic liposomes were prepared with the following ratio: anionic phospholipid/PC/Chol (10/10/1). Anionic phospholipids used were phosphatidylserine (PS), phosphatidylinositol (PI), phosphatidylglycerol (PG), or phosphatidic acid (PA). For anionic liposomes containing cardiolipin or cytidine diphosphate diacylglycerol (CDP-DAG), a ratio of 5/10/1 was used. This different ratio is necessary to get the same amount of charges for an equal concentration of total lipids. Chloroform was evaporated under vacuum. The lipid film was dissolved in 3 volumes of water-washed ether and 1 volume of 100 mM Tris and 136 mM NaCl, pH 7.4. Stable emulsion was obtained by sonication at room temperature. Ether was then evaporated for 20 min at 35 °C until obtaining a gel. Liposomes were formed after thoroughly vortexing of the gel. Separation of unincorporated lipids and residual ether was performed after dilution of the sample with 100 volumes of Tris buffer and ultracentrifugation at 25000 rpm for 1 h at 4 °C. Pelleted liposomes were resuspended in 100 mM Tris and 136 mM NaCl, pH 7.4.

Phospholipid Quantification. The total amount of lipids was determined upon quantification of the phosphate concentration by malachite green (*10*).

Binding of Peptides to Liposomes. All synthetic peptides contain at least one tryptophan residue, allowing monitoring of peptide transfer from the polar buffer to the membrane complex interface through the blue shift of fluorescence spectra (λ_{max} shift) (*11*). Increasing amounts of liposomes were added to a constant concentration of peptide (0.2 μM) in 100 mM Tris and 136 mM NaCl, pH 7.4. Tryptophans were excited at 280 nm, and fluorescence emission spectra were acquired between 290 and 450 nm on a FluoroMax-2 spectrofluorometer (Jobin Yvon-Spex). Quartz cuvettes (5 × 5 mm) and caps were precoated by 1% PEI during 1 h at room temperature in order to avoid peptide binding to cuvette walls. Background due to buffer and liposomes was subtracted with ORIGIN 6.0. The maximum emission wavelength (λ_{max}) was plotted as a function of lipid/peptide molar ratio. A decrease in λ_{max} (i.e., blue shift) indicates peptide binding to liposomes. Binding isotherms and partition coefficients were calculated as described (*12*).

Determination of Partition Coefficients. Partition coefficients were calculated as described (*12*). Briefly, binding isotherms were analyzed as a partition equilibrium using $X_b = K_p C_f$, where X_b is the molar ratio of bound peptide per total lipid, K_p is the partition coefficient, and C_f is the concentration of free peptide at equilibrium. The fraction of bound peptide was calculated using $f_b = (\lambda - \lambda_0)/(\lambda_\infty - \lambda_0)$. λ, λ_0, and λ_∞ are the wavelengths of maximum emission of

[1] Abbreviations: PEI, poly(ethylenimine); Fmoc, 9-fluorenylmethoxycarbonyl; PC, phosphatidylcholine; Chol, cholesterol; PS, phosphatidylserine; PI, phosphatidylinositol; PG, phosphatidylglycerol; PA, phosphatidic acid; CDP-DAG, cytidine diphosphate diacylglycerol; K_p, partition coefficient; K_{SV}(eff), Stern−Volmer constant.

fluorescence of bound peptide, free peptide, and peptide at saturation, respectively. X_b was then calculated using $P_T f_b$, where P_T is the total concentration of peptide and corrected as described by Beschiaschvili (*13*). X_b was plotted as a function of concentration of free peptide (C_f). The partition coefficient corresponds to the initial slope of the curve.

Acrylamide Fluorescence Quenching. This method was used to determine exposure of tryptophans of mitogaligin-derived peptides to solvent upon interaction with liposomes (*14*). Peptides, alone or in the presence of different liposome preparations, were incubated with increasing concentrations of acrylamide. Tryptophans were excited at 295 nm, and fluorescence emission spectra were obtained from 290 to 450 nm. Background related to buffer, acrylamide, and liposomes was subtracted. The ratio between fluorescence intensity without quencher (F_0) and fluorescence intensity in the presence of acrylamide quencher (F) was plotted against acrylamide concentration. The Stern−Volmer collisional quenching coefficient was determined as described (*14*) using the equation $F_0/F = 1 + K_{SV}(\text{eff})[Q]$ for collisional quenching, where K_{SV}(eff) is the Stern−Volmer quenching effective constant and [Q] is the concentration of the quencher. To take into account a static contribution to quenching, the modified Stern−Volmer equation was applied (*14*): $F_0/Fe^{V[Q]} = 1 + K_{SV}(\text{eff})[Q]$, where V is the static constant.

Peptide-Induced Aggregation of Liposomes. Aggregation of liposomes in the presence of peptides was measured after 15 min incubation by turbidimetry at 436 nm (*15*) with a UV−visible Varian Cary spectrometer. The maximum absorbance value was plotted as a function of peptide/phospholipid molar ratio.

Peptide-Induced Leakage of Liposome Contents. Leakage of liposome contents was monitored by the release of encapsulated [^{3}H]inulin. Three nanomoles of tritiated inulin ([^{3}H]inulin, 0.63 Ci/mmol; Amersham) was added to the aqueous phase during liposome preparation. Liposomes were washed and pelleted as described above. Radioactive liposomes were then incubated with increasing concentrations of peptides in 100 mM Tris and 136 mM NaCl, pH 7.4, for 1 h at 4 °C. Leakage was calculated after ultracentrifugation (25000 rpm for 1 h at 4 °C) by counting radioactivity associated with the supernatant and pellet with a liquid scintillation analyzer (Packard, Rungis, France). The leakage amount was obtained after normalization with untreated liposomes (0%) or dermaseptin S3-treated liposomes (100%). Dermaseptin has been shown to permeabilize liposomes (*12*).

Mitochondrial Aggregation. HeLa cells (10^6) were lysed in buffer A (220 mM mannitol, 68 mM sucrose, 10 mM Hepes−KOH, 70 mM KCl, 1 mM EDTA, 1 mM PMSF, 1 mM DTT, pH 7.7) for 30 min at 4 °C, dounced, and centrifuged (400*g*, 5 min). Supernatant was recentrifuged (15000*g*, 30 min). Pelleted mitochondria were resuspended in chilled buffer A and incubated with peptides at 62.5, 125, and 250 μM (30 min, 4 °C). Aggregation of mitochondria was measured by turbidimetry at 436 nm.

RESULTS

Delineation of the Mitogaligin Mitochondrial Targeting Signal. Previous experiments have shown that the mitochondrial localization sequence of mitogaligin is contained between amino acids 31 and 54 (*5*). In order to delineate more precisely this signal, cells were transfected with vectors encoding sequential deletions of this fragment fused to EGFP. Deletions were performed at the N- or C-terminal ends of the 31−54 sequence. Fluorescence microscopy observations of transfected cells show that the minimal mitochondrial targeting sequence of mitogaligin extends from arginine 31 to tryptophan 47 (Figure 2). Indeed, further deletions of residue arginine 31 or tryptophan 47 lead to cytosolic localization of the fusion protein. TMRM staining indicated that transfected and nontransfected cells displayed no major differences in the morphology of their mitochondria. However, TMRM labeling is often weaker and sometimes

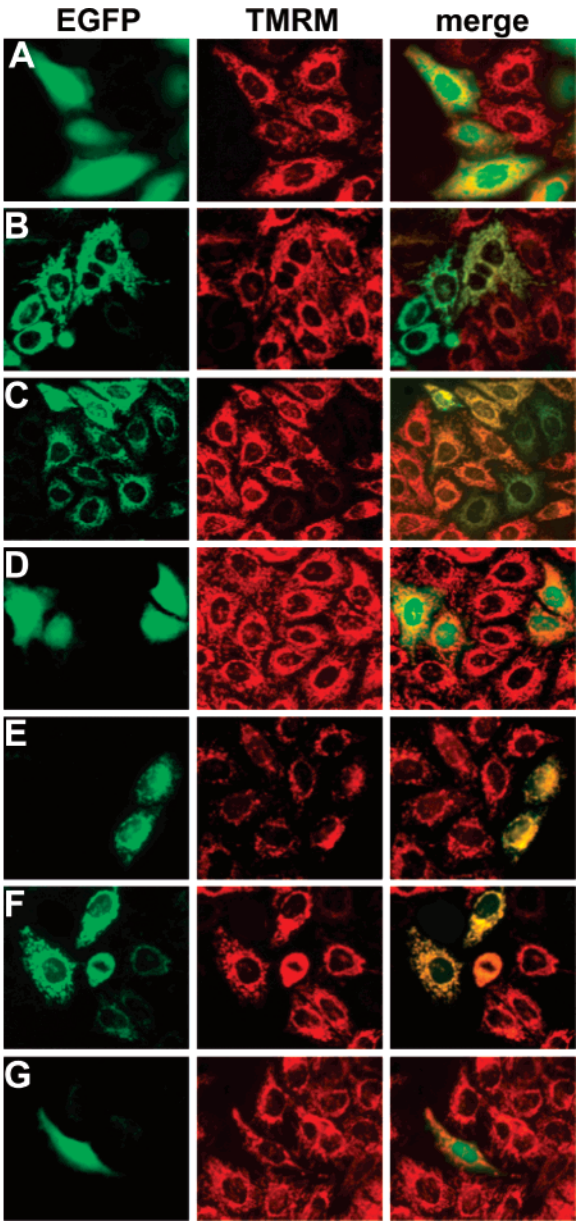

FIGURE 2: Determination of the mitochondrial-addressing signal of mitogaligin. HeLa cells were transfected with constructs encoding truncated forms of mitogaligin fused to EGFP and analyzed 24 h later by fluorescence microscopy for EGFP production (column EGFP) or mitochondrial staining with TMRM (column TMRM). Colocalization of mitogaligin-derived peptides and mitochondria was evaluated by merging the pictures (column merge). Vectors produce EGFP (A), full-length mitogaligin-EGFP (B), mitogaligin-[31−54]-EGFP (C), mitogaligin-[32−54]EGFP (D), mitogaligin-[31−48]-EGFP (E), mitogaligin-[31−47]-EGFP (F), and mitogaligin-[31−46]-EGFP (G).

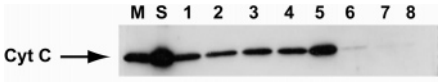

FIGURE 3: Release of mitochondrial cytochrome *c* upon transfection of plasmids encoding the mitochondrial targeting domain of mitogaligin. Cells were transfected with vectors encoding deleted forms of mitogaligin-EGFP containing a functional (lanes 1−5) or nonfunctional mitochondrial localization signal (lanes 6−8). Accumulation of cytosolic cytochrome *c* was analyzed by western blotting. Expression vectors produce intact mitogaligin (lane 1), mitogaligin-[31−54] (lane 2), mitogaligin-[31−47] (lane 3), mitogaligin-[31−48] (lane 4), mitogaligin-[31−49] (lane 5), mitogaligin-[32−54] (lane 6), mitogaligin-[31−46] (lane 7), and EGFP (lane 8). Lane M is horse cytochrome *c*, and lane S is supernatant from mitochondria treated with saponin.

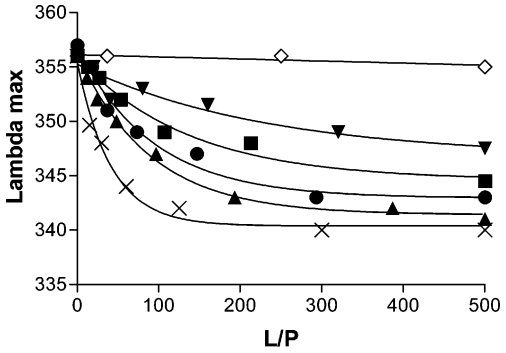

FIGURE 4: Titration of peptide MG-[31−53] by anionic liposomes. Measurements were realized by adding increasing amounts of phospholipids (L) to constant peptide concentration (200 nM) (P). The λ_{max} value of fluorescence was plotted against the L/P ratio. Liposomes were made of PC/Chol and anionic phospholipids, cardiolipin (×), PG (■), CDP-DAG (▲), PA (●), PI (▼), or PS (◇).

abolished in cells expressing peptides addressed to mitochondria, indicating a decrease in the mitochondrial membrane potential.

Transfection of Vectors Encoding the Mitogaligin Mitochondrial-Targeting Signal Induces Cytochrome c Release. In order to know whether mitochondrial destabilization is directly linked to the mitochondrial targeting sequence, accumulation of cytosolic cytochrome *c* was assayed upon transfection with vectors encoding deleted forms of mitogaligin-EGFP fusions (Figure 3). Prior to preparation of cell extracts, cells were checked by fluorescence microscopy for expression and correct localization of the hybrid proteins. Cytochrome *c* release was observed only when plasmids encoding a functional mitochondrial targeting sequence were used. Fusions of EGFP to 32−54 mitogaligin or 31−46 mitogaligin did not induce significant cytochrome *c* release. These results indicate that a complete signal is required to induce mitochondrial damage.

Preferential Binding of Mitogaligin-Derived Peptides to Lipid Vesicles Containing Cardiolipin. MG-[31−53], a synthetic peptide encompassing the mitochondrial targeting sequence of mitogaligin (Figure 1), was assayed for binding to liposomes by tryptophan fluorescence titration (*11*). When increasing amounts of zwitterionic liposomes (PC/Chol) were added to 200 nM peptide solutions, no shift of the maximum fluorescence emission wavelength of tryptophan was detected (data not shown). The same observation was made with anionic liposomes containing PS (Figure 4). These results reveal that MG-[31−53] has no or very low affinity for these neutral or negatively charged liposomes. At the contrary, blue

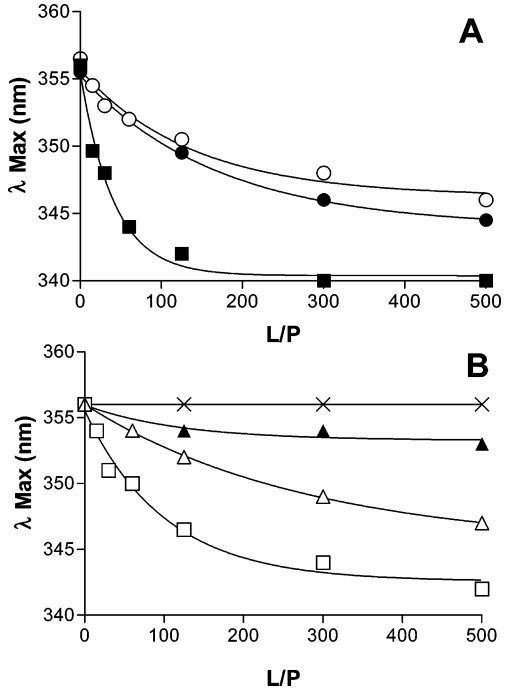

FIGURE 5: Titration of mitogaligin-derived peptides by cardiolipin-containing liposomes. PC/Chol/cardiolipin liposomes were incubated with (A) peptides MG-[31−53] (■), MG-[12−34] (●), and MG-[55 75] (○) and (B) peptide MG-[35−53] (□) and three analogues of MG-[35−53]: S39/E (△), T38S39/EE (▲), and R40R41/AA (×) (see Figure 1 for peptide sequences). The λ_{max} value of fluorescence was plotted against the lipid to peptide ratio (L/P) for P = 200 nM.

shifts were recorded upon titration with liposomes containing different anionic phospholipids. The highest affinity was observed for cardiolipin-containing liposomes (partition coefficient, $K_p = 10^{-6}$ M^{-1}). PI conferred much lower affinity than cardiolipin-containing liposomes ($K_p = 1.3 \times 10^{-7}$ M^{-1}). The phospholipids structurally related to cardiolipin (PG, $K_p = 1.8 \times 10^{-7}$ M^{-1}, CDP-DAG, $K_p = 3.4 \times 10^{-7}$ M^{-1}, and PA, $K_p = 2.9 \times 10^{-7}$ M^{-1}) displayed intermediate affinities. Since the experiments were realized using lipid compositions that maintain the same amount of negative charges, these differences in affinities are not entirely related to electrostatic contribution.

Two other mitogaligin-derived peptides were also tested for binding to cardiolipin-containing vesicles (Figure 5A). These peptides, MG-[12−34] and MG-[55−75], which did not include the mitochondrial targeting signal underwent a significant blue shift fluorescence emission. However, binding saturation of MG-[31−53] was reached for a much lower lipid to peptide (L/P) ratio, revealing a higher binding affinity for this peptide containing the mitochondrial targeting signal. Indeed, K_p for MG-[31−53], MG-[12−34], and MG-[55−75] are 10^{-6}, 0.26×10^{-6}, and 0.16×10^{-6} M^{-1}, respectively.

Electrostatic Contribution to Binding of Mitogaligin-Derived Peptides to Liposomes. Peptide−membrane interactions frequently result from a balance between electrostatic and hydrophobic interactions. To evaluate the electrostatic contribution in the binding of mitogaligin-derived peptides to cardiolipin-containing liposomes, peptides, initially designed to assess implications of putative phosphorylation sites (S39/E and T38S39/EE), were tested for their capacity to interact with synthetic membranes and compared to their

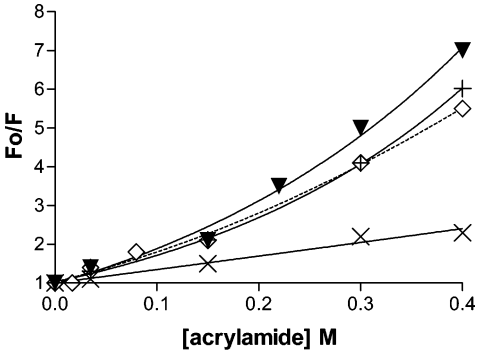

FIGURE 6: Fluorescence quenching by acrylamide. Increasing amounts of acrylamide were added to a constant concentration of MG-[31−53] in the absence (+) or in the presence of liposomes containing PC/Chol (▼), PC/PS/Chol (◇), or PC/cardiolipin/Chol (×). The ratio of lipid/peptide is 100. F_0 = fluorescence intensity without quenching. F = fluorescence intensity in the presence of acrylamide quencher.

parent peptide, MG-[35−53] ($K_p = 0.47 \times 10^{-6}$ M^{-1}) (Figure 5B). Substitution of hydroxylated residue S39 with negatively charged residue (E) led to peptides exhibiting marked decreases in blue shift, indicating a loss of interaction with liposomes ($K_p = 0.7 \times 10^{-7}$ M^{-1}) (Figure 5B). This effect was more pronounced for the disubstituted peptide T38S39/EE since binding was almost abolished. The effect of the reduction of the global charge of peptide MG-[31−53] was further investigated using the peptide R40R41/AA. Instead of adding negative charges to the peptide, the two arginines 40 and 41 were replaced with alanines, leading to a peptide with a net charge of +3. Although this peptide has the same global charge as the peptide S39/E, no blue shift or fluorescence emission was detected, indicating a more drastic inhibition.

Acrylamide Fluorescence Quenching of Mitogaligin-Derived Peptides. The acrylamide fluorescence quenching method was used to further characterize the interaction of MG-[31−53] with liposomes (Figure 6). Fluorescence of MG-[31−53] is very sensitive to quenching when the peptide is in a solution free of liposomes [K_{SV}(eff) = 8.1 M^{-1}]. A two-phase process can be observed. Quenching is linear for low concentrations of acrylamide, which is characteristic of collisional quenching (*14*). Higher concentrations induce upward curvature obtained classically for static quenching where collision is faster than the process of photon reemission. Very similar profiles (Figure 6) and Stern−Volmer constants were obtained in the presence of zwitterionic liposomes [K_{SV}(eff) = 8.7 M^{-1}] or anionic liposomes containing PS [K_{SV}(eff) = 8.3 M^{-1}]. This result is not surprising considering that little interaction was detected between this peptide and these liposomes. However, when cardiolipin-containing liposomes are used, quenching is linear over the range of acrylamide concentration and the quenching constant decreases largely [K_{SV}(eff) = 3.5 M^{-1}]. These results confirm the significant interaction of tryptophan residues of MG-[31−53] with the cardiolipin-containing membrane.

Liposome Aggregation by Mitogaligin-Derived Peptides. Because *galig* expression induces mitochondria aggregation, it was studied whether mitogaligin-derived peptides could be directly involved in this process. Aggregation of lipid vesicles was assayed by monitoring the turbidity of liposome suspension at 436 nm (Figure 7). Among the six peptides

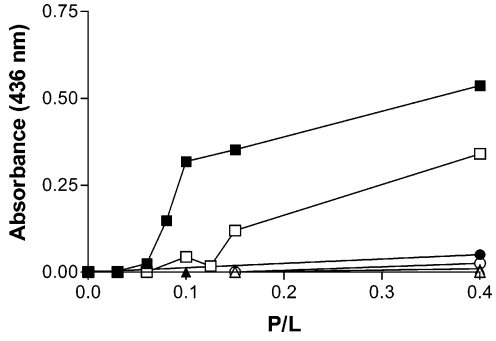

FIGURE 7: Aggregation of PC/cardiolipin/Chol liposomes was followed by measuring absorbance at 436 nm with increasing peptide/lipid ratio (P/L). The lipid concentration was maintained constant. Key: peptides MG-[31−53] (■), MG-[12−34] (●), MG-[55−75] (○), MG-[35−53] (□), S39/E (△), and T38S39/EE (▲) (see Figure 1 for peptide sequences).

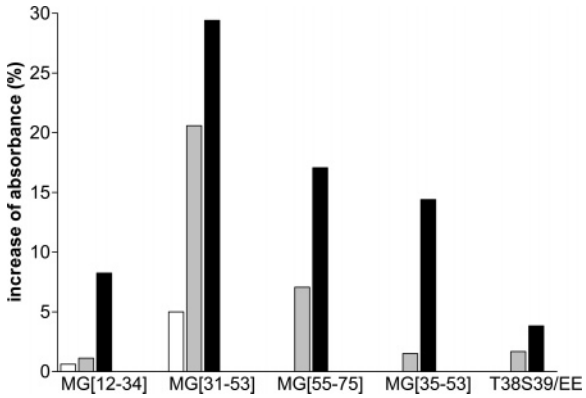

FIGURE 8: Aggregation of isolated mitochondria by peptides derived from mitogaligin. Isolated mitochondria were incubated with peptides at concentrations of 62.5 μM (white bars), 125 μM (gray bars), and 250 μM (black bars). Aggregation of mitochondria was followed by measuring absorbance at 436 nm. The *Y*-axis represents the increase of absorbance before and after addition of peptide to the mitochondria preparation.

added on liposomes containing cardiolipin, only two promoted liposome aggregation: MG-[31−53] and MG-[35−53], the latter being less efficient. No significant aggregation was observed with peptides MG-[12−34] or MG-[55−75] or with the two analogues of MG-[35−53] (S39/E and T38S39/EE). With anionic liposomes containing phosphatidylserine, only a slight aggregation could be observed for MG-[31−53] and only at higher peptide/lipid ratios (data not shown). Zwitterionic liposomes did not aggregate with any of the peptides (data not shown). As for binding experiments, liposome aggregation appears to be dependent on peptide sequence and lipid composition.

Aggregation of Isolated Mitochondria by Mitogaligin-Derived Peptides. Mitochondria were isolated from HeLa cells and incubated with increasing concentrations of the different peptides. Aggregation was assayed by monitoring the turbidity of mitochondria suspension at 436 nm (Figure 8) and checked by fluorescence microscopy (data not shown). Similarly to results obtained with synthetic membranes, mitochondria aggregation was the most efficient with MG-[31−53]. As expected, peptide MG-[35−53] exhibited less aggregation, and its mutant T38S39/EE showed no aggregation. A very weak aggregating activity was observed with MG-[12−34] and was barely visible under microscopy (data not shown). However, MG-[55−75] was as efficient as MG-

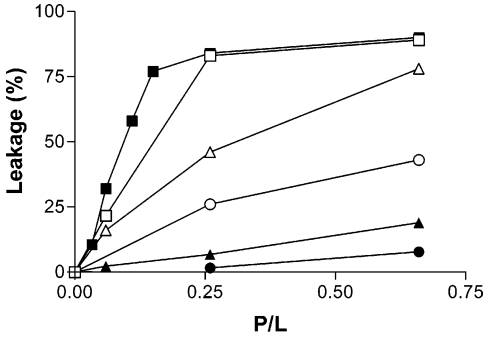

FIGURE 9: Liposome leakage assay. Permeabilization of PC/cardiolipin/Chol liposomes was evaluated by measuring the release of entrapped [^{3}H]inulin for increasing ratios of peptide/lipid (P/L). L is maintained constant. Key: peptides MG-[31−53] (■), MG-[12−34] (●), MG-[55−75] (○), MG-[35−53] (□), S39/E (△), and T38S39/EE (▲).

[35−53] in inducing aggregation of isolated mitochondria while it did not induce liposome aggregation.

Membrane Destabilization Activity of Peptides Derived from Mitogaligin. Membrane destabilization activity was evaluated by measuring the radioactivity released from [^{3}H]-inulin-containing liposomes incubated with increasing concentration of peptides (Figure 9). Zwitterionic liposomes did not leak with any of the peptides (data not shown). At the contrary, cardiolipin-containing liposomes were efficiently permeabilized with peptide MG-[31−53] and to a lesser extent with peptide MG-[35−53] (Figure 9). As expected from above data, destabilization was much more reduced for peptides MG-[12−34] and MG-[55−75]. Once again, the mono- or disubstituted analogue peptides MG-[35−53], S39/E and T38S39/EE, exhibited a lower permeabilizing activity as compared to their parent peptide MG-[35−53].

DISCUSSION

Galig expression was previously found to be cytotoxic when expressed in HeLa or MCF7 cells (*5*). Although the cell death pathway is not yet defined, typical markers of apoptosis can be evidenced such as loss of plasma membrane asymmetry, nucleic acid condensation, and cell shrinkage. It is now well established that disruption of mitochondria integrity constitutes frequently a key step of cell death (*1*−*4*, *16*). In this context, we have proposed that mitochondria play also a central role during the process of *galig*-induced cell death. Indeed, besides that *galig* encodes a mitochondrial protein named mitogaligin, the pivotal role of mitochondria in *galig* cytotoxicity is supported by the facts that *galig* expression promoted the release of mitochondrial cytochrome *c* and that Bcl-XL, a member of Bcl-2 family, inhibited *galig* induced cell death (*5*). Because mitogaligin is located at the mitochondria, we have undertaken the present study to evaluate the possible effects of mitogaligin on destabilization of the mitochondrial membrane.

The Mitochondrial-Targeting Sequence of Mitogaligin Binds to Anionic Phospholipids Related to Cardiolipin. Previous structure−activity relationship studies showed that the mitochondrial addressing of mitogaligin relies on an internal sequence bearing cytotoxicity (*5*). In this paper, the mitochondrial localization signal of mitogaligin has been precisely delineated by expressing truncated forms of mitogaligin fused to EGFP (Figure 2). Arginine 31 and tryptophan 47 border the minimal targeting sequence. This sequence has a typical amino acid composition of a mitochondrial signal characterized by enrichment in basic, hydrophobic, and hydroxylated residues (*17*). Binding assays of synthetic mitogaligin-derived peptides on liposomes confirmed that the central region containing the mitochondrial-addressing signal of mitogaligin is the major membrane-interacting sequence. However, the lipid binding activity is not strictly restricted to the addressing signal. Indeed, peptide MG-[35−53] lacks residues 31−34 and is not expected to be addressed to mitochondria. However, this peptide still binds to liposomes containing cardiolipin although less efficiently than MG-[31−53] (Figures 5B, 7, and 9). It is possible that mitogaligin needs a complete functional signal to be addressed to mitochondria but that interaction with synthetic lipid vesicles requires a minimum affinity. Indeed, the partition coefficient of MG-[35−53] is lower than that of MG-[31−53] but is higher than those of MG-[55−75] and MG-[12−34], which bind poorly to liposomes. Above all, binding to liposomes revealed that peptides interact directly with phospholipid membranes without any protein involvement (Figures 4 and 5). This binding relies on electrostatic interaction between cationic peptides and anionic phospholipids. Indeed, peptide analogues of MG-[35−53] with a reduced cationic net charge (T38S39/EE and S39/E) exhibited a decrease in membrane binding affinity. The peptide R40R41/AA, with the same global charge as S39/E, did not interact with liposomes containing cardiolipin, suggesting that the amino acid composition should also be taken into account. Consequently, the arginine doublet could play a critical role in this interaction.

Concerning the lipid partner, the anionic property of the phospholipid is not the unique feature driving this binding since PS liposomes do not interact with mitogaligin-derived peptides (Figure 4). In the same line of evidence, PI, another anionic phospholipid, showed only low-affinity binding. These results suggest that, besides the anionic property, binding requires the particular structural feature of the phospholipid. In that regard, it should be noted that phospholipids promoting high-affinity binding are structurally and metabolically related to cardiolipin, a phospholipid implicated in numerous vital functions such as respiration, ATP synthesis, mitochondrial protein import (*18*−*21*), and mitochondria-mediated cell death (*22*−*24*). Cardiolipin and its precursors are particularly concentrated at junctions between outer and inner mitochondrial membranes which might constitute anchor points for mitogaligin binding (*25*, *26*). In fact, cardiolipin and several anionic phospholipids have been shown to mediate binding of tBid, a proapoptotic member of the Bcl-2 family, through electrostatic and hydrophobic interactions (*27*, *28*). Interestingly, the preferential binding profile of mitogaligin to cardiolipin, PA, PG, and PI appeared to be very similar to that of tBid (*27*).

While not addressed in this paper, the possible effect of lipid curvature should also be considered. In the case of tBid, it has been shown that, in the presence of cardiolipin, leakage results from induction of negative membrane curvature (*29*). Replacement of cardiolipin with PG, which does not promote membrane curvature, prevents tBid from initiating leakage. In this regard, it is interesting to note that Bcl-X_L, an antiapoptotic protein which inhibits tBid activity by reducing

the promotion of nonbilayer phases (*29*), interferes also with cell death induced by *galig* expression (*5*).

In addition to electrostatic contributions, hydrophobic interactions participate to peptide binding as evidenced by quenching experiments showing that tryptophans interact significantly with the lipid bilayer (Figure 6). This may suggest a possible insertion of the peptide within the membrane but has to be confirmed by NMR. Fluorescence quenching is classically used to study the insertion of polypeptides within a lipid bilayer. However, in the case of tBid, although acrylamide fluorescence quenching suggests an insertion within the membrane, NMR reveals that the protein is in a parallel orientation with the membrane lipids (*30*).

The Mitochondrial-Targeting Sequence of Mitogaligin Induces Aggregation and Leakage of Mitochondria and Cardiolipin-Containing Vesicles. MG-[31−53], which covers the complete mitochondrial addressing signal, is the most effective peptide in aggregating cardiolipin-containing liposomes. This activity is dose-dependent on the peptide to lipid ratio (Figure 7). Interestingly, peptides issued from other regions of mitogaligin were not able to induce aggregation of liposomes. Similarly, MG-[31−53] strongly aggregates isolated mitochondria (Figure 8). This aggregation is associated with membrane damages as cytochrome *c* is released from these isolated mitochondria (*5*). However, it should be taken into account that the peptide MG-[55−75] and to a lesser degree MG-[12−34], while having no aggregating activity on liposomes, are able to promote some aggregation of isolated mitochondria. Consequently, we cannot exclude that, in addition to lipids, other factors facilitate aggregation of the mitochondrial membrane by mitogaligin-derived peptides.

These results reflect the clustering of mitochondria observed during cell death induced by *galig* expression (*5*). This aggregating activity is reminiscent of that observed with proapoptotic effectors such as tBid (*31*, *32*) or Bax (*33*). However, our data do not allow to conclude that the release of cytochrome *c* from mitochondria of *galig* transfected cells (*5*) and from cells expressing truncated forms of mitogaligin (Figure 3) is a direct consequence of mitochondria aggregation. Mitochondrial aggregation has been postulated to be an essential step for the cytochrome *c* release in mitochondria-dependent cell death (*34*, *35*). However, it is now more prevalent that other morphological changes such as mitochondrial fission and cristae remodeling are primary events leading to cytochrome *c* release (*36*, *37*). Further investigation will be necessary to evaluate the possible implication of mitogaligin or mitogaligin-derived peptides in these events.

Given the in vitro observation that peptides derived from mitogaligin induce mitochondrial aggregation, it may be surprising that no difference in mitochondria morphology was noticeable in vivo upon cell transfection (Figure 2). However, when peptides are addressed to mitochondria, TMRM labeling, which is sensitive to mitochondrial membrane potential (*38*), is often weaker or even abolished, thus indicating a loss of mitochondrial membrane integrity. A comparable situation is also observed after transfection of the *galig* gene. Aggregation appears lately several hours after production of the protein (ref *5* and unpublished results). This difference in the rate of mitochondria aggregation in vivo and in vitro could be related to the concentration of peptides/protein. The intracellular concentration of peptides or protein upon gene transfection may be low when compared to in vitro experiments. Indeed, when peptide MG-[35−53] is microinjected in the cytosol, aggregation is immediate while MG-[12−34] has little effect and MG-[55−75] has no effect (*5*).

Experiments with liposomes show that direct interaction between anionic lipids and the mitochondrial addressing peptide of mitogaligin is necessary for aggregation and leakage (Figures 7 and 9). However, the precise mechanism of cytochrome *c* release remains to be elucidated. It should be noted that, in vivo, the release of cytochrome *c* after transfection of the truncated forms of mitogaligin is limited. The major part of cytochrome *c* remains associated with mitochondria pellets (data not shown). Such an observation was also made with the cardiolipin binding domain of tBid which, by itself, can suppress mitochondrial respiration by interaction with cardiolipin. This isolated sequence can also induce cytochrome *c* release but was much less potent that tBid (*39*). It has been postulated that this may be related to the absence of a BH3 domain. Similarly, it is possible that, in addition to the cardiolipin binding domain of mitogaligin, other sequences are required to obtain complete dissociation and release of cytochrome *c*.

As postulated for tBid, mitogaligin, upon binding to cardiolipin, could dissociate the cardiolipin−cytochrome *c* complex also stabilized by electrostatic and hydrophobic interactions (*19*, *40*, *41*). This would allow cytochrome *c* release in the intermembranous space of mitochondria (*42*). Leakage from mitochondria would concomitantly result from a lipid phase transition to hexagonal phase II of cardiolipin (*29*, *43*). However, this functional similarity is not related to a structural homology. The structure of the tBid-cardiolipin binding domain has been elucidated and consists of three α helices (*27*, *47*). Analysis of the mitogaligin sequence by different prediction programs reveals no secondary structures. Nevertheless, it is possible that the lipid environment affects folding and that mitogaligin and mitogaligin-derived peptides acquired their final structure upon binding to the membrane. This study is under current investigation.

Mitogaligin has a structure rich in cationic residues (12% arginine) and in tryptophans (12%). Although no sequence homology was found with any other known proteins, including proteins from the Bcl-2 family, such amino acid composition is reminiscent of Trp-rich cationic antimicrobial peptides such as indolicidin, tritrpticin, and lactoferricin derivatives (*45*−*47*). Such cytotoxic peptides are known to destabilize anionic membranes (*48*, *49*).

Altogether, the results presented in this paper show that mitogaligin is a new cell death effector which interacts with mitochondrial phospholipids related to cardiolipin and induces mitochondrial membrane destabilization and leakage of cytochrome *c*. The exact mechanism of cytochrome *c* release remains to be elucidated though it could present similarity with that of some antimicrobial peptides.

ACKNOWLEDGMENT

We are grateful to Dr. Agnès Delmas (CNRS, Centre de Biophysique Moléculaire, Orléans, France) for guidance on peptide synthesis.

REFERENCES

1. Green, D. R., and Evan, G. I. (2002) A matter of life and death, *Cancer Cell 1*, 19−30.
2. Newmeyer, D. D., and Ferguson-Miller, S. (2003) Mitochondria: releasing power for life and unleashing the machineries of death, *Cell 112*, 481−490.
3. Bouchier-Hayes, L., Lartigue, L., and Newmeyer, D. D. (2005) Mitochondria: pharmacological manipulation of cell death, *J. Clin. Invest. 115*, 2640−2647.
4. Martinou, J. C., and Green, D. R. (2001) Breaking the mitochondrial barrier, *Nat. Rev. Mol. Cell. Biol. 2*, 63−67.
5. Duneau, M., Boyer-Guittaut, M., Gonzalez, P., Charpentier, S., Normand, T., Dubois, M., Raimond, J., and Legrand, A. (2005) Galig, a novel cell death gene that encodes a mitochondrial protein promoting cytochrome *c* release, *Exp. Cell Res. 302*, 194−205.
6. Guittaut, M., Charpentier, S., Normand, T., Dubois, M., Raimond, J., and Legrand, A. (2001) Identification of an internal gene to the human Galectin-3 gene with two different overlapping reading frames that do not encode Galectin-3, *J. Biol. Chem. 276*, 2652−2657.
7. Boussif, O., Lezoualc'h, F., Zanta, M. A., Mergny, M. D., Scherman, D., Demeneix, B., and Behr, J. P. (1995) A versatile vector for gene and oligonucleotide transfer into cells in culture and in vivo: polyethylenimine, *Proc. Natl. Acad. Sci. U.S.A. 92*, 7297−7301.
8. King, D. S., Fields, C. G., and Fields, G. B. (1990) A cleavage method which minimizes side reactions following Fmoc solid phase peptide synthesis, *Int. J. Pept. Protein Res. 36*, 255−266.
9. Delmotte, C., Le, Guern, E., Trudelle, Y., and Delmas, A. (1999) Structural features of a chimeric peptide inducing cytotoxic T lymphocyte responses in saline, *Eur. J. Biochem. 265*, 336−345.
10. Zhou, X., and Arthur, G. (1992) Improved procedures for the determination of lipid phosphorus by malachite green, *J. Lipid Res. 33*, 1233−1236.
11. Ladokhin, A. S., Jayasinghe, S., and White, S. H. (2000) How to measure and analyze tryptophan fluorescence in membranes properly, and why bother?, *Anal. Biochem. 285*, 235−245.
12. Pouny, Y., Rapaport, D., Mor, A., Nicolas, P., and Shai, Y. (1992) Interaction of antimicrobial dermaseptin and its fluorescently labeled analogues with phospholipid membranes, *Biochemistry 31*, 12416−12423.
13. Beschiaschvili, G., and Seelig, J. (1990) Melittin binding to mixed phosphatidylglycerol/phosphatidylcholine membranes, *Biochemistry 29*, 52−58.
14. Eftink, M. R., and Ghiron, C. A. (1976) Exposure of tryptophanyl residues in proteins. Quantitative determination by fluorescence quenching studies, *Biochemistry 15*, 672−680.
15. Persson, D., Thoren, P. E., and Norden, B. (2001) Penetratin-induced aggregation and subsequent dissociation of negatively charged phospholipid vesicles, *FEBS Lett. 505*, 307−312.
16. Kuwana, T., and Newmeyer, D. D. (2003) Bcl-2-family proteins and the role of mitochondria in apoptosis, *Curr. Opin. Cell Biol. 15*, 691−699.
17. Truscott, K. N., Brandner, K., and Pfanner, N. (2003) Mechanisms of protein import into mitochondria, *Curr. Biol. 13*, R326−R337.
18. Weiss, C., Oppliger, W., Vergeres, G., Demel, R., Jeno, P., Horst, M., de Kruijff, B., Schatz, G., and Azem, A. (1999) Domain structure and lipid interaction of recombinant yeast Tim44, *Proc. Natl. Acad. Sci. U.S.A. 96*, 8890−8894.
19. Demel, R. A., Jordi, W., Lambrechts, H., van Damme, H., Hovius, R., and de Kruijff, B. (1989) Differential interactions of apo- and holocytochrome *c* with acidic membrane lipids in model systems and the implications for their import into mitochondria, *J. Biol. Chem. 264*, 3988−3997.
20. Ou, W. J., Ito, A., Umeda, M., Inoue, K., and Omura, T. (1988) Specific binding of mitochondrial protein precursors to liposomes containing cardiolipin, *J. Biochem. (Tokyo) 103*, 589−595.
21. Jiang, F., Ryan, M. T., Schlame, M., Zhao, M., Gu, Z., Klingenberg, M., Pfanner, N., and Greenberg, M. L. (2000) Absence of cardiolipin in the crd1 null mutant results in decreased mitochondrial membrane potential and reduced mitochondrial function, *J. Biol. Chem. 275*, 22387−22394.
22. Garcia Fernandez, M., Troiano, L., Moretti, L., Nasi, M., Pinti, M., Salvioli, S., Dobrucki, J., and Cossarizza, A. (2002) Early changes in intramitochondrial cardiolipin distribution during apoptosis, *Cell Growth Differ. 13*, 449−455.
23. Petrosillo, G., Ruggiero, F. M., and Paradies, G. (2003) Role of reactive oxygen species and cardiolipin in the release of cytochrome *c* from mitochondria, *FASEB J. 17*, 2202−2208.
24. Kagan, V. E., Tyurin, V. A., Jiang, J., Tyurina, Y. Y., Ritov, V. B., Amoscato, A. A., Osipov, A. N., Belikova, N. A., Kapralov, A. A., Kini, V., Vlasova, II, Zhao, Q., Zou, M., Di, P., Svistunenko, D. A., Kurnikov, I. V., and Borisenko, G. G. (2005) Cytochrome *c* acts as a cardiolipin oxygenase required for release of proapoptotic factors, *Nat. Chem. Biol. 1*, 223−232.
25. Ardail, D., Privat, J. P., Egret-Charlier, M., Levrat, C., Lerme, F., and Louisot, P. (1990) Mitochondrial contact sites. Lipid composition and dynamics, *J. Biol. Chem. 265*, 18797−18802.
26. Boya, P., Roques, B., and Kroemer, G. (2001) New EMBO members' review: viral and bacterial proteins regulating apoptosis at the mitochondrial level, *EMBO J. 20*, 4325−4331.
27. Lutter, M., Fang, M., Luo, X., Nishijima, M., Xie, X., and Wang, X. (2000) Cardiolipin provides specificity for targeting of tBid to mitochondria, *Nat. Cell Biol. 2*, 754−761.
28. Zha, J., Weiler, S., Oh, K. J., Wei, M. C., and Korsmeyer, S. J. (2000) Posttranslational N-myristoylation of BID as a molecular switch for targeting mitochondria and apoptosis, *Science 290*, 1761−1765.
29. Epand, R. F., Martinou, J. C., Fornallaz-Mulhauser, M., Hughes, D. W., and Epand, R. M. (2002) The apoptotic protein tBid promotes leakage by altering membrane curvature, *J. Biol. Chem. 277*, 32632−32639.
30. Gong, X. M., Choi, J., Franzin, C. M., Zhai, D., Reed, J. C., and Marassi, F. M. (2004) Conformation of membrane-associated proapoptotic tBid, *J. Biol. Chem. 279*, 28954−28960.
31. Li, H., Zhu, H., Xu, C. J., and Yuan, J. (1998) Cleavage of BID by caspase 8 mediates the mitochondrial damage in the Fas pathway of apoptosis, *Cell 94*, 491−501.
32. Zhai, D., Miao, Q., Xin, X., and Yang, F. (2001) Leakage and aggregation of phospholipid vesicles induced by the BH3-only Bcl-2 family member, BID, *Eur. J. Biochem. 268*, 48−55.
33. Desagher, S., and Martinou, J. C. (2000) Mitochondria as the central control point of apoptosis, *Trends Cell Biol. 10*, 369−377.
34. Takada, S., Shirakata, Y., Kaneniwa, N., and Koike, K. (1999) Association of hepatitis B virus X protein with mitochondria causes mitochondrial aggregation at the nuclear periphery, leading to cell death, *Oncogene 18*, 6965−6973.
35. Haga, N., Fujita, N., and Tsuruo, T. (2003) Mitochondrial aggregation precedes cytochrome *c* release from mitochondria during apoptosis, *Oncogene 22*, 5579−5585.
36. Youle, R. J., and Karbowski, M. (2005) Mitochondrial fission in apoptosis, *Nat. Rev. Mol. Cell. Biol. 6*, 657−663.
37. Cereghetti, G. M., and Scorrano, L. (2006) The many shapes of mitochondrial death, *Oncogene 25*, 4717−4724.
38. Scaduto, R. C., Jr., and Grotyohann, L. W. (1999) Measurement of mitochondrial membrane potential using fluorescent rhodamine derivatives, *Biophys. J. 76*, 469−477.
39. Liu, J., Weiss, A., Durrant, D., Chi, N. W., and Lee, R. M. (2004) The cardiolipin-binding domain of Bid affects mitochondrial respiration and enhances cytochrome *c* release, *Apoptosis 9*, 533−541.
40. Nicholls, P. (1974) Cytochrome *c* binding to enzymes and membranes, *Biochim. Biophys. Acta 346*, 261−310.
41. Cortese, J. D., Voglino, A. L., and Hackenbrock, C. R. (1998) Multiple conformations of physiological membrane-bound cytochrome *c*, *Biochemistry 37*, 6402−6409.
42. Ott, M., Robertson, J. D., Gogvadze, V., Zhivotovsky, B., and Orrenius, S. (2002) Cytochrome *c* release from mitochondria proceeds by a two-step process, *Proc. Natl. Acad. Sci. U.S.A. 99*, 1259−1263.
43. Seddon, J. M., Kaye, R. D., and Marsh, D. (1983) Induction of the lamellar-inverted hexagonal phase transition in cardiolipin by protons and monovalent cations, *Biochim. Biophys. Acta 734*, 347−352.
44. Chou, J. J., Li, H., Salvesen, G. S., Yuan, J., and Wagner, G. (1999) Solution structure of BID, an intracellular amplifier of apoptotic signalling, *Cell 96*, 615−624.
45. Bellamy, W., Takase, M., Yamauchi, K., Wakabayashi, H., Kawase, K., and Tomita, M. (1992) Identification of the bactericidal domain of lactoferrin, *Biochim. Biophys. Acta 1121*, 130−136.

46. Selsted, M. E., Novotny, M. J., Morris, W. L., Tang, Y. Q., Smith, W., and Cullor, J. S. (1992) Indolicidin, a novel bactericidal tridecapeptide amide from neutrophils, *J. Biol. Chem. 267*, 4292−4295.
47. Lawyer, C., Pai, S., Watabe, M., Borgia, P., Mashimo, T., Eagleton, L., and Watabe, K. (1996) Antimicrobial activity of a 13 amino acid tryptophan-rich peptide derived from a putative porcine precursor protein of a novel family of antibacterial peptides, *FEBS Lett. 390*, 95−98.
48. Nissen-Meyer, J., and Nes, I. F. (1997) Ribosomally synthesized antimicrobial peptides: their function, structure, biogenesis, and mechanism of action, *Arch. Microbiol. 167*, 67−77.
49. Papo, N., and Shai, Y. (2003) Can we predict biological activity of antimicrobial peptides from their interactions with model phospholipid membranes?, *Peptides 24*, 1693−1703.

BI700213P